Experimental evidence on the origin of Ca-rich carbonated melts formed by interaction between sedimentary limestones and mantle-derived ultrabasic magmas

Lustrino, Michele; Luciani, Natascia; Stagno, Vincenzo; Narzisi, Silvia; Masotta, Matteo; Scarlato, Piergiorgio

published in
Geology
2022

DOI (link to publisher)
10.1130/G49621.1

document version
Publisher's PDF, also known as Version of record

GEOLOGY | THE GEOLOGICAL SOCIETY OF AMERICA®

https://doi.org/10.1130/G49621.1

Manuscript received 24 August 2021
Revised manuscript received 17 October 2021
Manuscript accepted 24 October 2021

Published online 5 January 2022

Experimental evidence on the origin of Ca-rich carbonated melts formed by interaction between sedimentary limestones and mantle-derived ultrabasic magmas

Michele Lustrino[1,2]*, Natascia Luciani[1,3], Vincenzo Stagno[1,4], Silvia Narzisi[1], Matteo Masotta[5] and Piergiorgio Scarlato[4]
[1]Dipartimento di Scienze della Terra, Sapienza Università di Roma, Piazzale Aldo Moro, 5, 00185 Rome, Italy
[2]Consiglio Nazionale delle Ricerche Istituto di Geologia Ambientale e Geoingegneria (IGAG), c/o Dipartimento di Scienze della Terra, Sapienza Università di Roma, Piazzale Aldo Moro, 5, 00185 Rome, Italy
[3]Faculty of Science, Vrije Universiteit Amsterdam, De Boelelaan 1085, 1081 HV Amsterdam, Netherlands
[4]Istituto Nazionale di Geofisica e Vulcanologia, Sezione di Roma 1, Via di Vigna Murata, 605, 00143 Rome, Italy
[5]Dipartimento di Scienze della Terra, Università degli Studi di Pisa, Via S. Maria, 53, 56126 Pisa, Italy

ABSTRACT

In this experimental study, we documented the formation of strongly ultrabasic and ultracalcic melts through the interaction of melilititic and basanitic melts with calcite. Three strongly to moderately SiO_2-undersaturated volcanic rocks from the Bohemian Massif (central Europe) were mixed with 10, 30, and 50 wt% $CaCO_3$ and melted at 1100, 1200, and 1300 °C at 2 kbar to evaluate the maximum amount of carbonate that can be assimilated by natural ultrabasic melts at shallow depths. Experiments revealed a surprisingly complete dissolution of the $CaCO_3$, only rarely reaching carbonate saturation, with typical liquidus phases represented by olivine, spinel, melilite, and clinopyroxene. Only in the runs with the most SiO_2-undersaturated compositions did abundant monticellite form instead of clinopyroxene. For all starting mixtures, strongly ultrabasic (SiO_2 down to 15.6 wt%), lime-rich (CaO up to 43.6 wt%), ultracalcic (CaO/Al_2O_3 up to ~27) melt compositions were produced at 1200 and 1300 °C, with up to ~25 wt% dissolved CO_2. When present, quenched olivine showed much higher forsterite content ($Fo_{95–97}$) than olivine in the natural samples ($Fo_{79–85}$). The two major results of this study are (1) silicate-carbonatite melt compositions do not necessarily imply the existence of carbonatitic components in the mantle, because they are also produced during limestone assimilation, and (2) Fo-rich olivines cannot be used to infer any primitive character of the melt nor high potential temperature (T_p).

INTRODUCTION

Near-solidus partial melting of a carbonated mantle produces carbonatitic liquids (e.g., Hammouda and Keshav, 2015). An increase of the melting degree results in a more diluted carbonate component, due to the increasing contribution of the partial melts derived from the silicate matrix. As a result, melts with a broad spectrum of compositions can be produced, varying from nearly pure carbonatitic (i.e., without SiO_2) to basaltic (Gudfinnsson and Presnall, 2005; Green, 2015; Yaxley et al., 2019; Weidendorfer et al., 2020; Keshav and Gudfinnsson, 2021).

A secondary, but frequently overlooked mechanism for the origin of carbonatitic magmas has little relation to upper-mantle dynamics. Indeed, carbonatite melts can be produced at crustal depths via sedimentary carbonate anatexis caused by hydrothermal fluids with high $H_2O/(H_2O + CO_2)$ (~0.95; Lentz, 1999) released by deep-seated solidifying magmas. The interaction between carbonatite (both mantle- and crustal-derived) and silicate components leads to the formation of a group of poorly characterized compositions, classified as silicocarbonatites (Le Maitre, 2002; Mitchell, 2005). Hybrid compositions can result after the assimilation of sedimentary carbonates by ultrabasic melts (e.g., Lustrino et al., 2019, 2020; Sklyarov et al., 2021) or, vice versa, assimilation of crustal silicate rocks by carbonatitic to ultrabasic-ultracalcic CO_2-bearing melts (e.g., Ackerman et al., 2021). In this experimental study, we documented the formation of silicate-carbonatite melts through the interaction between basaltic melts *sensu lato* and limestones and dolostones. Large amounts of CO_2 can be dissolved at crustal depths and then abruptly released through simple upwelling, cooling, and crystallization magma mechanisms.

MATERIALS AND METHODS

Three compositionally distinct volcanic rocks from the Bohemian Massif (central Europe) were used as starting material for carbonate-melt interaction experiments (Table 1): (1) a Paleocene melilite-olivine-nephelinite (polzenite, sampled on the Great Devil's Wall, Osečná Complex, Czech Republic) with ~38.5 wt% SiO_2 (sample BM1); (2) a Paleocene monticellite-bearing melilitite (vesecite, at the type locality Vesec village, Czech Republic) with ~30.3 wt% SiO_2 (sample BM2); and (3) an olivine basanite (collected at the village of Jauernick, near the town of Görlitz, Germany) with ~43 wt% SiO_2 (sample BM3). The composition of the three volcanic rocks resembles mafic melts in equilibrium with a peridotitic assemblage, being characterized by high contents of MgO (15.9–17.1 wt%), Ni (300–440 ppm), and Cr (710–1010 ppm), and with Mg# ~74 (assuming $Fe^{3+}/\Sigma Fe = 0.15$).

Each starting material was subjected to two cycles of melting at 1400 and 1450 °C for up to 12 h, quenching as glass, and powdering, and was then mixed with 10, 30, and 50 wt% of reagent-grade $CaCO_3$ and inserted in platinum capsules. In total, 41 isobaric experiments were performed at 2 kbar in a non-end-loaded piston cylinder, using standard 1 inch (2.54 cm) low-pressure assemblies (Masotta et al., 2012).

*E-mail: michele.lustrino@uniroma1.it

CITATION: Lustrino, M., et al., 2022, Experimental evidence on the origin of Ca-rich carbonated melts formed by interaction between sedimentary limestones and mantle-derived ultrabasic magmas: Geology, v. 50, p. 476–480, https://doi.org/10.1130/G49621.1

TABLE 1. NATURAL SAMPLES AND QUENCHED GLASSES USED FOR EXPERIMENTS.

Run number	*T* (°C)	*P* (kbar)	$CaCO_3$ added (wt%)	SiO_2	TiO_2	Al_2O_3	FeO	MnO	MgO	CaO	Na_2O	K_2O	P_2O_5	Total	CO_2 (100 – total)	CaO/Al_2O_3	Mg#
BM1 (natural sample; polzenite)				38.52	2.86	9.85	11.20	0.18	15.94	13.58	2.75	1.82	1.15	97.84	2.2	1.4	0.73
BM1 (quenched glass)			0	40.11	3.00	9.66	9.98	0.17	15.94	13.40	2.88	1.73	1.09	98.09	1.9	1.4	0.75
QP1_123_10	1100	2	10	38.87	2.54	10.94	7.57	0.18	5.88	22.93	3.90	2.66	1.25	96.73	3.3	2.10	0.59
QP1_123_30	1100	2	30	31.25	1.24	6.73	4.29	0.12	2.92	29.54	3.60	3.51	1.93	85.13	14.9	4.39	0.56
QP1_123_50	1100	2	50	29.49	1.23	3.98	2.05	0.14	4.57	40.40	3.36	2.08	0.73	88.03	12.0	10.15	0.81
QP1_125_10	1200	2	10	37.19	2.77	9.69	8.80	0.16	10.88	20.20	2.91	1.82	1.13	95.56	4.4	2.08	0.70
QP1_125_30	1200	2	30	33.21	2.43	7.89	6.91	0.14	11.33	26.56	2.42	1.55	0.98	93.42	6.6	3.37	0.76
QP1_125_50	1200	2	50	29.34	2.15	5.91	5.48	0.13	10.46	31.33	2.19	1.36	0.89	89.23	10.8	5.30	0.78
QP1_124_10	1300	2	10	37.40	2.55	8.95	9.30	0.15	14.26	18.61	2.62	1.65	1.03	96.52	3.5	2.08	0.74
QP1_124_30	1300	2	30	33.26	2.28	7.71	7.60	0.14	12.67	25.88	2.41	1.47	1.00	94.41	5.6	3.36	0.76
QP1_124_50	1300	2	50	29.78	2.00	6.88	6.42	0.14	11.54	30.52	2.11	1.30	0.89	91.57	8.4	4.43	0.77
BM2 (natural sample; vesecite)				30.29	2.27	7.39	11.25	0.20	17.10	21.96	0.93	0.74	1.46	93.59	6.4	3.0	0.74
BM2 (quenched glass)			0	32.84	2.44	7.68	11.12	0.22	18.23	22.82	1.06	0.74	1.66	98.80	1.2	2.97	0.76
RM41_10	1200	2	10	30.70	2.50	6.56	6.44	0.19	10.80	30.16	1.23	0.78	1.99	91.35	8.6	4.60	0.76
RM41_30	1200	2	30	21.69	1.75	2.83	3.15	0.18	8.21	38.80	1.64	1.15	2.25	81.64	18.4	13.73	0.83
RM41_50	1200	2	50	15.62	1.45	1.62	2.40	0.12	6.92	43.58	1.05	0.81	1.34	74.90	25.1	26.89	0.84
RM37_10	1300	2	10	30.13	2.17	6.10	7.71	0.19	14.39	29.19	1.01	0.69	1.57	93.14	6.9	4.79	0.78
RM37_30	1300	2	30	24.79	1.67	3.98	5.11	0.15	12.08	36.25	0.79	0.51	1.28	86.59	13.4	9.12	0.82
RM37_50	1300	2	50	17.83	1.23	1.99	2.97	0.12	8.42	43.37	0.53	0.37	0.96	77.81	22.2	21.76	0.84
BM3 (natural sample; basanite)				43.92	1.94	10.91	11.61	0.17	16.93	10.49	2.35	1.00	0.55	99.87	0.1	1.0	0.73
BM3 (quenched glass)			0	44.95	2.00	10.81	10.70	0.19	16.86	10.21	2.47	1.00	0.68	99.84	0.2	0.94	0.75
RM44_10	1100	2	10	44.58	2.22	10.05	7.82	0.09	11.91	20.81	1.24	0.32	0.47	99.51	0.5	2.07	0.74
RM44_30	1100	2	30	42.38	0.17	6.15	2.03	0.05	12.60	33.79	0.51	0.28	0.21	98.16	1.8	5.49	0.92
RM44_50	1100	2	50	16.51	1.52	2.19	2.24	0.12	6.01	43.47	1.85	0.94	0.73	75.57	24.4	19.85	0.84
RM43_10	1200	2	10	42.63	2.00	10.92	8.69	0.18	11.41	17.95	2.44	0.96	0.60	97.78	2.2	1.64	0.71
RM43_30	1200	2	30	35.76	1.52	8.31	6.48	0.14	11.45	28.20	1.88	0.78	0.51	95.04	5.0	3.39	0.77
RM43_50	1200	2	50	26.10	1.09	5.13	3.16	0.07	8.94	38.69	1.33	0.54	0.36	85.40	14.6	7.54	0.84
RM42_10	1300	2	10	41.74	1.89	10.65	9.39	0.15	12.44	16.94	2.31	0.96	0.54	97.01	3.0	1.59	0.71
RM42_30	1300	2	30	35.85	1.48	8.19	7.08	0.12	12.93	27.27	1.85	0.73	0.44	95.94	4.1	3.33	0.78
RM42_50	1300	2	50	26.85	1.08	5.74	4.67	0.09	9.41	37.90	1.33	0.50	0.35	87.92	12.1	6.60	0.79

Note: Values for major oxides are given in wt%. Mg# = 100 × Mg/(Mg + Fe^{2+}) assuming $Fe^{3+}/\Sigma Fe = 0.15$.

The pressure of 2 kbar was selected to mimic the interaction between silicate melts and the base of the overthickened limestone thrusts of the Central Apennines, located at a depth of ~5–6 km (Barchi et al., 2003). Mixtures were maintained at temperatures of 1100, 1200, and 1300 °C for 1–12 h and then quenched (Table 1). Full details on the analytical techniques and bulk analyses of natural rocks and experimental compositions (including mineral compositions) are provided in the Supplemental Material[1].

RESULTS

Vesicles were common in all the experimental runs, thereby indicating the attainment of CO_2 saturation in all the residual melts. Runs carried out at 1100 °C were either subsolidus or characterized by compositionally heterogeneous glass pools. Runs carried out at 1200 °C and 1300 °C were characterized by large patches of homogeneous glass containing scarce quench crystals, and, for this reason, these runs were used to constrain the composition of the hybrid melts. The most important compositional changes of the experiments are presented below in order of increasing SiO_2 content of the starting material.

BM2 Experiments

Only the experiment doped with 50 wt% of $CaCO_3$ at 1300 °C was supraliquidus (except for a minor amount of quench crystals of calcite). All the other experiments crystallized Ca-rich (CaO ~2.0–2.5 wt%) and Mg-rich olivine ($Fo_{96–97}$) always associated with minor monticellite ($La_{35–47}$; Mg# = 84–94) and Al-Fe-Mg spinel (occasionally chromite-rich) ± melilite. No substantial chemical differences among the glasses quenched at 1200 °C and 1300 °C were observed (Fig. 1). The experiments performed at 1300 °C showed a negative correlation between all the major oxides of the melt and $CaCO_3$ added, with very high coefficients of determination [R^2 varying from 0.94 (FeO_{tot}) to 1.00 (Al_2O_3)]. The amount of CaO in the residual melt and the estimated CO_2 content (i.e., 100 – glass weight percent total from the microprobe analyses) showed a positive correlation with the amount of $CaCO_3$ added ($R^2 = 0.99$ for both oxides). The SiO_2 content ranged from ~30 wt% to ~16 wt%, while CaO increased from ~23 wt% to ~44 wt% with increasing $CaCO_3$ added.

BM1 Experiments

Runs at 1100 °C did not crystallize olivine, but abundant kushiroite-rich (Al_2O_3 = 9.4–10.6 wt%) clinopyroxene, melilite, and spinels were observed, also with calcite ± perovskite. Olivine ($Fo_{95–97}$; CaO = 1.1–2.8 wt%), Al-rich clinopyroxene (Al_2O_3 = 7.7–10.6 wt%), and spinel were present in all the experiments at 1200 °C and 1300 °C, with calcite found only in experiments doped with 30 wt% and 50% $CaCO_3$. Also in this case, the 1200 °C and 1300 °C runs produced residual melts with nearly indistinguishable compositions (Fig. 1). Major oxides showed negative correlations with the amount of $CaCO_3$ added, with R^2 mostly clustering around 0.94–0.99. Experiments carried out at 1200 °C showed lower R^2 with $CaCO_3$, likely due to subliquidus conditions and the selective removal of specific oxides by nearby quenched minerals (e.g., see the drop of MgO in charges doped with 10 wt% $CaCO_3$, likely related to strong MgO incorporation in olivine). As the amount of $CaCO_3$ increased, the concentration of SiO_2 in the residual melt decreased from ~40.0 wt% to ~29.8 wt%. At the same time, CaO of the residual melt increased from ~13.4 wt% to 30.5 wt%, coupled with an increase of CO_2 from ~1 to ~9 wt%.

BM3 Experiments

Residual melts obtained at 1200 °C and 1300 °C showed similar major-oxide compositions, again defining a nearly perfect negative correlation with the amount of $CaCO_3$ added to the starting material (R^2 = 0.96–1.00). As reported above, the concentration of CaO in the melt was also perfectly correlated with the amount of $CaCO_3$ added ($R^2 = 1.00$). However, the estimated amount of CO_2 was less correlated with $CaCO_3$ ($R^2 = 0.76$), perhaps due to CO_2 lost in the abundant vesicles. The oxides of BM3 and BM1 glasses showed a nearly complete overlap, except for TiO_2, which was more abundant in the BM3 starting composition. The modal content of olivine ($Fo_{94–97}$) tended to decrease with increasing $CaCO_3$, due to the enlargement of the clinopyroxene and melilite stability fields.

[1]Supplemental Material. Experimental and analytical procedures, including SEM images of the experimental runs, and a data set containing the entire set of EMP analyses of glass and quenched minerals, as well as the original composition of the starting materials and additional plots. Please visit https://doi.org/10.1130/GEOL.S.17139341 to access the supplemental material, and contact editing@geosociety.org with any questions.

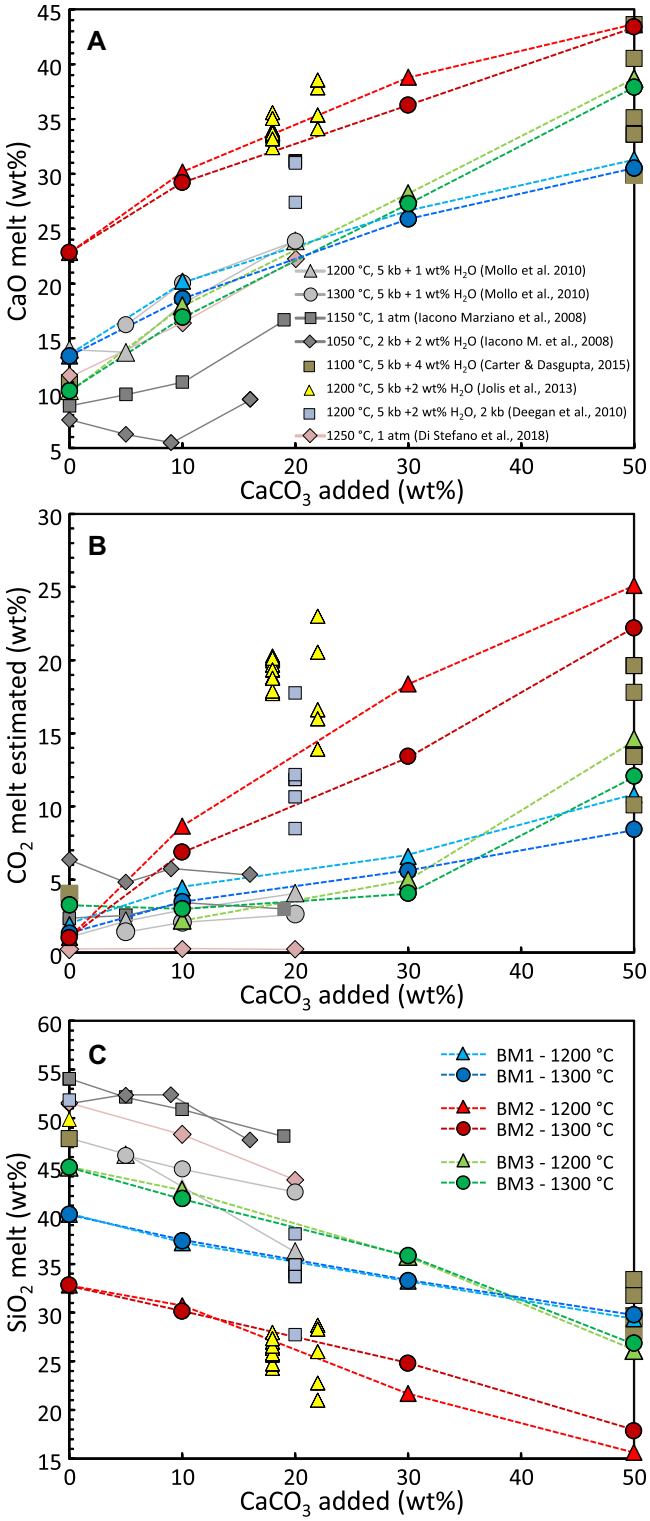

Figure 1. (A) CaO, (B) CO_2, and (C) SiO_2 in experimental glasses obtained at 1200 and 1300 °C versus $CaCO_3$ added. Literature experiments mixing $CaCO_3$ with natural and synthetic basaltic compositions are reported for comparison.

DISCUSSION

Maximum Amount of Carbonate Assimilation by a Natural Melt

CaO- and MgO-rich ultracalcic and ultrabasic compositions are interpreted in the literature as the result of low-degree partial melting of carbonated peridotite sources (e.g., Hammouda and Keshav, 2015; Lustrino et al., 2021). However, experimental melts from this study document that these kinds of ultracalcic and ultrabasic compositions can be easily obtained by magma-carbonate interaction at crustal depths. In particular, while previous studies focused on the assimilation of carbonate material by basaltic melts (Iacono Marziano et al., 2008; Mollo et al., 2010; Carter and Dasgupta, 2015; Di Stefano et al., 2018) to andesitic-dacitic melts (Carter and Dasgupta, 2016), our experiments were carried out on natural ultrabasic and strongly silica-undersaturated melts.

Figure 1 shows the increase of CaO and CO_2, as well as the decrease of SiO_2 content, in the melt as a function of the amount of $CaCO_3$, showing a good agreement with literature data from similar experiments. Literature compositions reach carbonate saturation at contents of <20 wt% of $CaCO_3$ added, as proved by the presence of quenched calcite crystals in the experimental runs (Mollo et al., 2010; Jolis et al., 2013). Carter and Dasgupta (2015) reported the presence of variable amounts of quenched glass (~9 to ~69 vol%) associated with abundant calcite (~26 to ~50 vol%) and other minerals (i.e., clinopyroxene, plagioclase, spinel, and scapolite, in order of lower abundance). This phase assemblage testifies to prolonged calcite saturation for a 1:1 mixture of a synthetic basalt and $CaCO_3$ equilibrated at 1100–1200 °C and 5–10 kbar. In contrast, our results only rarely reached carbonate saturation, as evidenced by the presence of minute amounts (<5 vol% of the capsule) of calcite microlites.

Experiments from the literature are characterized by higher degrees of crystallization of Ca-Mg-Al-Fe–rich clinopyroxene (e.g., Iacono Marziano et al., 2008; Mollo et al., 2010) during carbonate assimilation. This leads to the formation of residual melts depleted in SiO_2 and enriched in alkalis. These chemical variations were not observed in our experiments, where only CaO and the estimated CO_2 increased in the residual melt as the added $CaCO_3$ increased.

Changes in Olivine Crystal Chemistry

The key chemical features of olivine crystallized from $CaCO_3$-doped melts are summarized in Figure 2, where the maximum CaO and the maximum Fo contents of olivine are plotted as function of $CaCO_3$ added to the experimental charge. The maximum CaO content in olivine was 2.84 wt%, 2.21 wt%, and 2.46 wt% for BM2 (vesecite), BM1 (polzenite), and BM3 (basanite), respectively (Fig. 2A). Our results showed an increase in CaO content in olivine only for the BM1 and BM3 compositions (Fig. 2A), whereas the Fo content remained more or less unchanged in all the experiments (Fig. 2B) with increasing $CaCO_3$. This partially contrasts with the results reported in previous works (Iacono Marziano et al., 2008; Mollo et al., 2010; Di Stefano et al., 2018).

Overall, the increasing solubility of CaO in the melt favors Ca incorporation in the M2 site of olivine, thereby increasing the Ca → Fe^{2+} substitutions (Di Stefano et al., 2018). On the other hand, Mg in the M1 site of olivine increases with increasing $CaCO_3$ assimilation due to the fact that Ca cations are incorporated in the M2 site only. The result-

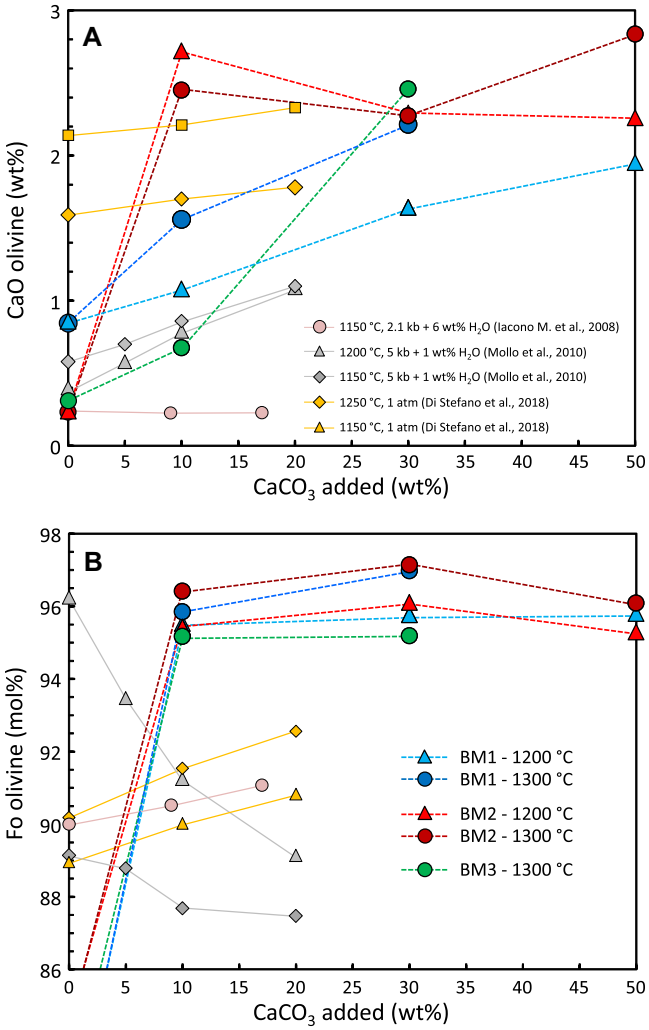

Figure 2. (A) $CaO_{olivine}$ (wt%) and (B) $Fo_{olivine}$ versus $CaCO_3$ added (wt%) in experimental melts obtained by adding variable amounts of $CaCO_3$. Olivine compositions of starting samples (BM1, BM2, and BM3) are reported for comparison.

ing effect is an increase of the Fo content in olivine, as already experimentally noted (Jolis et al., 2013; Di Stefano et al., 2018) and found in natural systems (e.g., Lustrino et al., 2019). The constant high forsterite content of the quenched olivines indicates a sort of saturation of Ca-Fe-Mg ions in the M1 and M2 sites. The value of partition coefficient $KD(Fe\text{-}Mg)^{olivine/melt}$ calculated to equilibrate Fo_{96} olivine in equilibrium with a Mg# = 77–84 melt (~0.15–0.24) is much lower than the expected equilibrium range between olivine and basaltic melts (0.27–0.39). This conclusion is opposite to what is observed for natural ultrabasic-ultracalcic systems (e.g., Lustrino et al., 2021). As a consequence, high-Fo olivine crystals can be no longer considered as an indicator of primitive magma compositions, nor for the elevated potential temperature (T_p) of crystallizing magmatic systems.

CONCLUSIONS

The effects of the addition of 10, 30, and 50 wt% $CaCO_3$ on three different natural SiO_2-undersaturated compositions were investigated at 2 kbar and 1100, 1200, and 1300 °C. We demonstrated that, upon availability of the energy required for the assimilation of crustal material (i.e., heating of crustal rocks to melting temperature and latent heat of fusion), up to 50 wt% of $CaCO_3$ can be assimilated by SiO_2-ultrabasic liquids, producing strongly SiO_2-ultrabasic (SiO_2 down to 15.6 wt%) ultracalcic melts (CaO/Al_2O_3 = 1.6–26.9). The major-oxide content of these melts varied as a function of the dilution by the CaO and CO_2 components and eventual mineral saturation. The resulting ultracalcic melts were extremely poor in SiO_2 (maximum CIPW normative larnite = 19.3 wt%) and rich in MgO (average 11.9 ± 2.0 wt%) and had an Mg# (71–84) proportional to the amount of $CaCO_3$ assimilated. These compositional changes are particularly relevant to interpretations of the genesis of some ultrabasic compositions cropping out in central Italy (e.g., Polino, San Venanzo, Cupaello volcanoes; Lustrino et al., 2011), although the implications can be exported to all igneous crustal settings where mafic magmas are in contact with thick carbonate systems.

The main conclusions from this experimental study are:

(1) Ultrabasic magmas can assimilate limestone up to a 1:1 ratio, reaching only minimum amounts of calcite saturation.

(2) Olivine is the liquidus phase in $CaCO_3$-doped, strongly ultrabasic magmas, replaced or joined by clinopyroxene and melilite in $CaCO_3$-doped, mildly ultrabasic magmas.

(3) Monticellite rims develop around Ca-rich olivine crystals when strongly SiO_2-undersaturated melts assimilate carbonate (as, for example, recorded at Polino volcano in central Italy; Lustrino et al., 2019).

(4) Olivine crystallizing from $CaCO_3$-doped ultrabasic magmas is characterized by strongly forsteritic compositions (up to Fo_{97}), a feature that shares more similarities with skarn than with alleged primitive magma compositions generated at high T_p.

(5) The $KD(Fe\text{-}Mg)^{olivine/melt}$ calculated in this study (~0.15–0.24) is lower than that observed for natural basaltic systems (~0.3; Roeder and Emslie, 1970) and much lower than that measured or calculated for carbonatitic and ultracalcic-ultrabasic compositions (>0.4–0.5; Dalton and Wood, 1993; Lustrino et al., 2021).

(6) The maximum inferred CO_2 content in the $CaCO_3$-doped melt reaches ~25 wt%, a feature that can have a strong impact on the eruptive styles of natural systems, because it can abruptly exsolve when magma approaches the surface, giving rise to violent paroxysms.

(7) The presence of CaO- and CO_2-rich magmas, as well as primary carbonate crystallization or the presence of immiscible carbonate-silicate droplets, and the presence itself of carbonatitic magma are features not necessarily related to the presence of a carbonated mantle.

ACKNOWLEDGMENTS

We thank M. Serracino and M. Albano (CNR–IGAG, Rome) for assistance during electron microprobe (EMP) and scanning electron microscope work. Thanks to Silvio Mollo (Rome) for his availability to discuss basic concepts of magma-limestone assimilation. PRIN 2017 Project 20177BX42Z_005 and Ateneo La Sapienza grants (2019–2020) are deeply appreciated. The revisions proposed by Giada Iacono Marziano (Orléans, France) and Oleg Safonov (Černogolovka, Russia) contributed to improve the readability of the manuscript. M. Lustrino thanks Jörg Büchner for providing the BM3 sample; the organizers of the excellent Conference Basalt 2013 at the Senckenberg Museum of Natural History, Görlitz, Germany, for the great excursion during which Lustrino collected the samples; Vladislav Rapprich and Ondřej Pour (Prague) for providing olivine EMP analyses of Great Devil's Wall (BM1 sample); and Mike Stern for his little shoes.

REFERENCES CITED

Ackerman, L., Rapprich, V., Polak, L., Magna, T., Mclemore, V.T., Pour, O., and Cejkova, B., 2021, Petrogenesis of silica-rich carbonatites from continental rift settings: A missing link between carbonatites and carbonated silicate melts?: Journal of Geosciences (Prague), v. 66, p. 71–87, https://doi.org/10.3190/jgeosci.320.

Barchi, M., Minelli, G., Magnani, B., and Mazzotti, A., 2003, Line CROP 03: Northern Apennines,

in Scrocca, D., et al., eds., CROP Atlas: Seismic Reflection Profiles of the Italian Crust: Memorie Descrittive della Carta Geologica d'Italia 62, p. 127–136.

Carter, L.B., and Dasgupta, R., 2015, Hydrous basalt–limestone interaction at crustal conditions: Implications for generation of ultracalcic melts and outflux of CO_2 at volcanic arcs: Earth and Planetary Science Letters, v. 427, p. 202–214, https://doi.org/10.1016/j.epsl.2015.06.053.

Carter, L.B., and Dasgupta, R., 2016, Effect of melt composition on crustal carbonate assimilation: Implications for the transition from calcite consumption to skarnification and associated CO_2 degassing: Geochemistry Geophysics Geosystems, v. 17, p. 3893–3916, https://doi.org/10.1002/2016GC006444.

Dalton, J.A., and Wood, B.J., 1993, The compositions of primary carbonate melts and their evolution through wallrock reaction in the mantle: Contributions to Mineralogy and Petrology, v. 119, p. 511–525.

Deegan, F.M., Troll, V.R., Freda, C., Misiti, V., Chadwick, J.P., McLeod, C.L., and Davidson, J.P., 2010, Magma-carbonate interaction processes and associated CO_2 release at Merapi volcano, Indonesia: Insights from experimental petrology: Journal of Petrology, v. 51, p. 1027–1051, https://doi.org/10.1093/petrology/egq010.

Di Stefano, F., Mollo, S., Scarlato, P., Nazzari, M., Bachmann, O., and Caruso, M., 2018, Olivine compositional changes in primitive magmatic skarn environments: A reassessment of divalent cation partitioning models to quantify the effect of carbonate assimilation: Lithos, v. 316–317, p. 104–121, https://doi.org/10.1016/j.lithos.2018.07.008.

Green, D.H., 2015, Experimental petrology of peridotites, including effects of water and carbon on melting in the Earth's upper mantle: Physics and Chemistry of Minerals, v. 42, p. 95–122, https://doi.org/10.1007/s00269-014-0729-2.

Gudfinnsson, G.H., and Presnall, D.C., 2005, Continuous gradations among primary carbonatitic, kimberlitic, melilititic, basaltic, picritic, and komatiitic melts in equilibrium with garnet lherzolite at 3–8 GPa: Journal of Petrology, v. 46, p. 1645–1659, https://doi.org/10.1093/petrology/egi029.

Hammouda, T., and Keshav, S., 2015, Melting in the mantle in the presence of carbon: Review of experiments and discussion on the origin of carbonatites: Chemical Geology, v. 418, p. 171–188, https://doi.org/10.1016/j.chemgeo.2015.05.018.

Iacono Marziano, G., Gaillard, F., and Pichavant, M., 2008, Limestone assimilation by basaltic magmas: An experimental re-assessment and application to Italian volcanoes: Contributions to Mineralogy and Petrology, v. 155, p. 719–738, https://doi.org/10.1007/s00410-007-0267-8.

Jolis, E.M., Freda, C., Troll, V.R., Deegan, F.M., Blythe, L.S., McLeod, C.L., and Davidson, J.P., 2013, Experimental simulation of magma-carbonate interaction beneath Mt. Vesuvius, Italy: Contributions to Mineralogy and Petrology, v. 166, p. 1335–1353, https://doi.org/10.1007/s00410-013-0931-0.

Keshav, S., and Gudfinnsson, G.H., 2021, A reappraisal of peridotite solidus phase equilibria from 6 to 14 GPa in the system CaO-MgO-Al_2O_3-SiO_2: Journal of Petrology, v. 62, p. egab009, https://doi.org/10.1093/petrology/egab009.

Le Maitre, R.W., ed., 2002, Igneous Rocks: A Classification and Glossary of Terms (2nd ed.): Cambridge, UK, Cambridge University Press, 236 p., https://doi.org/10.1017/CBO9780511535581.

Lentz, D.R., 1999, Carbonatite genesis: A reexamination of the role of intrusion-related pneumatolytic skarn processes in limestone melting: Geology, v. 27, p. 335–338, https://doi.org/10.1130/0091-7613(1999)027<0335:CGAROT>2.3.CO;2.

Lustrino, M., Duggen, S., and Rosenberg, C.L., 2011, The central-western Mediterranean: Anomalous igneous activity in an anomalous collisional setting: Earth-Science Reviews, v. 104, p. 1–40, https://doi.org/10.1016/j.earscirev.2010.08.002.

Lustrino, M., Luciani, N., and Stagno, V., 2019, Fuzzy petrology in the origin of carbonatitic/pseudocarbonatitic Ca-rich ultrabasic magma at Polino (central Italy): Scientific Reports, v. 9, 9212, https://doi.org/10.1038/s41598-019-45471-x.

Lustrino, M., Ronca, S., Caracausi, A., Bordenca, C.V., Agostini, S., and Faraone, D.B., 2020, Strongly SiO_2-undersaturated, CaO-rich kamafugitic Pleistocene magmatism in central Italy (San Venanzo volcanic complex) and the role of shallow depth limestone assimilation: Earth-Science Reviews, v. 208, 103256, https://doi.org/10.1016/j.earscirev.2020.103256.

Lustrino, M., Salari, G., Rahimzadeh, B., Fedele, L., Masoudi, F., and Agostini, S., 2021, Quaternary melanephelinites and melilitites from Nowbaran (NW Urumieh-Dokhtar magmatic arc, Iran): Origin of ultrabasic-ultracalcic melts in a post-collisional setting: Journal of Petrology, v. 62, p. egab058, https://doi.org/10.1093/petrology/egab058.

Masotta, M., Freda, C., Paul, T.A., Moore, G.M., Gaeta, M., Scarlato, P., and Troll, V.R., 2012, Low pressure experiments in piston cylinder apparatus: Calibration of newly designed 25 mm furnace assemblies to $P = 150$ MPa: Chemical Geology, v. 312–313, p. 74–79, https://doi.org/10.1016/j.chemgeo.2012.04.011.

Mollo, S., Gaeta, M., Freda, C., Di Rocco, T., Misiti, V., and Scarlato, P., 2010, Carbonate assimilation in magmas: A reappraisal based on experimental petrology: Lithos, v. 114, p. 503–514, https://doi.org/10.1016/j.lithos.2009.10.013.

Roeder, P.L., and Emslie, R.F., 1970, Olivine-liquid equilibrium: Contributions to Mineralogy and Petrology, v. 29, p. 275–289.

Sklyarov, E.V., Lavrenchuk, A.V., Doroshkevich, A.G., Starikova, A.E., and Kanakin, S.V., 2021, Pyroxenite as product of mafic-carbonate melt interaction (Tazheran Massif, west Baikal area, Russia): Minerals (Basel), v. 11, p. 654, https://doi.org/10.3390/min11060654.

Weidendorfer, D., Manning, C.E., and Schmidt, M.W., 2020, Carbonate melts in the hydrous upper mantle: Contributions to Mineralogy and Petrology, v. 175, p. 72, https://doi.org/10.1007/s00410-020-01708-x.

Yaxley, G.M., Ghosh, S., Kiseeva, E.S., Mallik, A., Spandler, C., Thomson, A.R., and Walter, M.J., 2019, CO2-rich melts in Earth, *in* Orcutt, B.N., et al., eds., Deep Carbon: Past to Present: Cambridge, UK, Cambridge University Press, p. 129–162, https://doi.org/10.1017/9781108677950.

Printed in USA